UDK 669.14.018.62
Original scientific article/Izvirni znanstveni članek

ISSN 1580-2949
MTAEC9, 56(2)193(2022)

SPINODAL DECOMPOSITION OF PRECIPITATION HARDENING Fe-17Cr-4Ni-4Cu STAINLESS STEEL AT 475 °C

SPINODALNI RAZPAD IZLOČEVALNO UTRJENEGA NERJAVNEGA JEKLA Fe-17Cr-4Ni-4Cu PRI 475 °C

Xue Ma[1], Zhijun Wang[2], Xuezhu Tong[1], Xiaoming Du[1]*, Tianfu Li[2], Rongdeng Liu[2], Yuntao Liu[2], Dongfeng Chen[2]

[1]School of Materials Science and Engineering, Shenyang Ligong University, Shenyang ,China
[2]China Institute of Atomic Energy, Beijing, China

Prejem rokopisa – received: 2021-12-13; sprejem za objavo – accepted for publication: 2022-02-22

doi:10.17222/mit.2021.336

Microstructure evolution and mechanical properties in an Fe-17Cr-4Ni-4Cu alloy aged at 475 °C after different aging times were studied. Conventional transmission electron microscopy (TEM) and high-resolution electron microscopy (HREM) studies revealed the formation of 9R-structure Cu-rich precipitates and Cr-rich α' phase by spinodal decomposition in the samples aged at 475 °C after 100–1000 h. The fine Cu-rich precipitates and Cr-rich α' phase by spinodal decomposition lead to a significant increase in the hardness, together in the early stages (100 h). Continued aging to 500 h leads to increased precipitation of the Cr-rich α', which provides significant strengthening, reaching maximum hardening, despite the continued loss of hardening by weakening by the Ostwald ripening of the Cu-rich precipitates. Extending the aging time to 1000 h leads to substantial reversed austenite transformation and a large number of ripening ε-copper precipitates that causes softening. The results of the impact tests showed that the major fracture mode was cleavage and/or quasi-cleavage.

Keywords: stainless steel, age hardening, spinodal decomposition, Cu-rich phase

Avtorji so študirali razvoj mikrostrukture in mehanskih lastnosti jeklene litine Fe-17Cr-4Ni-4Cu starane pri različnih časih na temperaturi 475 °C. Izvajali so konvencionalno presevno elektronsko mikroskopijo (TEM) in elektronsko mikroskopijo z visoko ločljivostjo (HREM) staranih vzorcev. Preiskave so pokazale, da prihaja do tvorbe 9R strukture bogate z izločki Cu in faze α' bogate s Cr med spinodalnim razpadom vzorcev staranih pri 475 °C po 100 h do 1000 h. Drobni izločki Cu in α' faze bogate s Cr po spinodalnem razpadu vodi istočasno do pomembnega zvišanja trdote zlitine že po relativno kratkem času staranja (po 100 h). Nadaljnje podaljševanje časa staranja (do 500 h) povzroča pospešeno izločanje s Cr bogate faze α', ki povzroča pomembno utrjevanje zlitine do maksimalne vrednosti zaradi kontinuirnega zmanjševanja učinka mehčanja zlitine, ki ga povzroča Ostwaldovo zorenje (rast) izločkov bogatih z Cu. Podaljševanje časa staranja do 1000 h vodi do pomembne reverzibilne austenitne transformacije in nastajanja velikega števila Cu izločkov ε, kar povzroča mehčanje zlitine. Preiskusi udarne žilavosti in posnetki prelomov na vrstičnem elektronskem mikroskopu (SEM) so pokazali, da med lomom staranih vzorcev prihaja predvsem do dveh mehanizmov loma in sicer cepilnega in/ali kvazi cepilnega.

Ključne besede: nerjavno jeklo, staranje, spinodalni razpad, faza bogata z bakrom

1 INTRODUCTION

Precipitation-hardened stainless steel is a kind of stainless steel with high strength and certain corrosion resistance obtained by the precipitation of fine intermetallic compounds and a few carbides during the aging process, which was widely used in aerospace, nuclear industry, petroleum, chemical and energy and other fields.[1–3] So it has received extensive attention from researchers. The precipitation-hardened stainless steels are of three types, *i.e.*, martensitic, semi-austenitic and austenitic, based on their martensite start and finish temperatures and resultant behaviour upon cooling from a suitable solution-treatment temperature.[4] At present, precipitation-hardened stainless steel parts are often used for the safety valves in nuclear reactors. For such applications, they face a severe problem of embrittlement due to the precipitation of the Cr-rich α' phases in the range 300–500 °C.[5] After long-term service, the loss of impact toughness and ductility is often observed, which can lead to the component being ruined.[6] Therefore, exploring the changes in the structure and mechanical properties of precipitation-hardened stainless steel during the aging process is more beneficial to the selection and use of stainless steel.[7,8]

It is well known that in Fe-Cr alloys there is a miscibility gap, where the ferrite phase may decompose into an Fe-enriched BCC phase (α) and a Cr-enriched BCC phase (α') either by one of the following two mechanisms: nucleation and growth of α' precipitates or by spinodal decomposition.[9] The former mechanism develops via the formation of α' particles in the α matrix, while the latter mechanism develops via a spontaneous de-mixing of Fe and Cr with an interconnected network of concentration fluctuations, leading to a two-phase nanostructure of α and α'.[10] It should be noted that after long aging times, the lattice mismatch between the α and α' phases generated by the decomposition, causes the

*Corresponding author's e-mail:
du511@163.com

elastic strain fields that cause an increased hardness but decreased toughness of the Fe-Cr alloys. In addition, for Fe-Cr-Ni-Cu alloys, the formation of Cu-rich precipitates is considered to be the primary hardening mechanism, hence the development of this nanostructure has also been intensively studied.[11,12] Wei You et al. believed that the increase in hardness and yield strength of 17-4PH stainless steel after aging at 400 °C for a long time was mainly due to the precipitation of fcc-Cu in the δ-ferrite phase.[13] Jun Wang et al. studied the aging of 17-4PH martensitic stainless steel at 350°C for a long time, and found that spinodal decomposition first occurred at the grain boundary, and the spinodal decomposition gradually changed from grain boundary to intragranular with the extension of time.[14] Yrieix and Guttmann reported that 17-4 PH stainless steel exhibits high susceptibility to aging embrittlement at 400 °C , and they concluded that it was essentially due to α' precipitation.[15] In their study, however, no microstructural observation results were shown.

The purpose of this work is to investigate the effect of the evolution of microstructure on hardening behavior of the Fe-17Cr-4Ni-4Cu alloy during aging at 475 °C up to 1000 h. The extent of degradation was characterized by impact and microhardness tests. TEM and HREM were used to examine the microstructural evolution during aging.

2 EXPERIMENTAL PART

2.1 Materials and heat treatments

The alloys used in this study with a composition of 17 *w*/% Cr, 4.8 *w*/% Ni, 3.5 *w*/% Cu and balance Fe were melted in a vacuum induction furnace from high-purity materials: 99.99 *w*/% Fe, 99.9 *w*/% Cr, 99.99 *w*/% Cu and 99.98 *w*/% Ni. The ingot was homogenized at 1100 °C for 3 h, hot forged between 1150 °C and 900 °C into 40-mm-thick slabs, and hot-rolled with a starting temperature of 1000 °C into 15-mm-thick strips. The hot-rolled sheet was then cut into (15 × 15 × 9.5) mm blocks. The blocks were annealed at 1050 °C for 2 h and immediately oil-quenched to produce a random solid solution. The aging treatments were performed on the specimens for (100, 500 and 1000) h at 475 °C in air. The aging temperature was controlled to ± 2 °C.

2.2 Specimens for tests and observation

The mechanical properties of the specimens with and without aging were determined by Charpy V-notch impact tests, Vickers hardness tests at room temperature. The (10 × 10 × 55) mm specimen with 2-mm V-notch according to ASTM E23 standard were tested on an instrumented 300 J Charpy impact testing machine. Hardness tests were made by using a Vickers hardness tester (with a load of 1 kg applied for 15 s). Hardness measurements were periodically obtained throughout the aging process, and aging continued until the hardness stopped increasing.

2.3 Microstructure characterization

The metallographic microstructures of the Fe-17Cr-4Ni-4Cu alloy after thermal aging were observed using TEM (FEI TecnaiG20) and HREM (FEI TecnaiG20), which were both operated at 200 kV. Thin foils for the TEM observations were cut from the samples, mechanically ground to a thickness of approximately 60 μm, and thinned using a twin-jet polishing system at 20 °C using a solution of 5 % perchloric acid and 95 % ethanol. X-ray diffraction (XRD) analyses on polished samples were carried out with a Rigaku Ultima IV) using Cu–K_α radiation for 20–100 degrees. Raw XRD data were refined and analyzed via MDI Jade 6.0 program (Materials Data Incorporated: Livermore, CA, USA). Fractography of the impact specimens was performed in a scanning electron microscope (SEM) of S-3400N.

3 RESULTS AND DISCUSSION

3.1 Age-hardening behavior

The variation in Vickers hardness of the specimens at heat-treatment temperature as a function of holding time is shown in **Figure 1**. The value at 0 represents the hardness after solution treatment and oil quenching. The error is the standard deviation after averaging over 5 measurements. It can be seen that the alloy exhibits significant precipitation hardening behavior at 475 °C. A marked hardness increase from 272.6–376.4 HV occurs from 0–100 h. At later times, the hardness remains steady up to 500 h. A decreasing trend is only observed after the measurement at 500 h. The overall hardening behavior is similar to the results reported by Guma for 17-4 PH stainless steel for long-term aging at 480 °C, for which a peak in hardness was observed after aging for

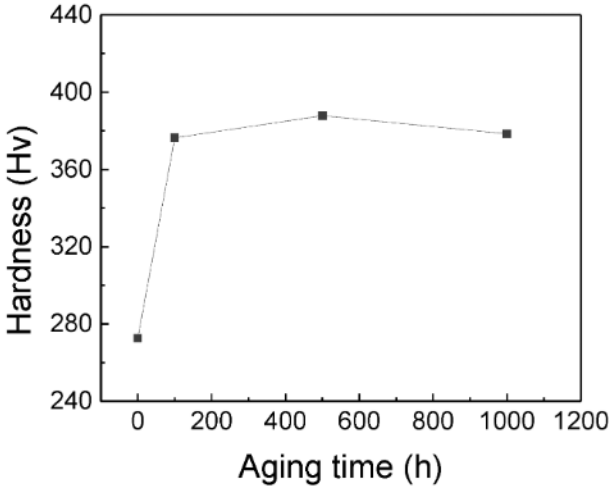

Figure 1: Hardening behavior of Fe-17Cr-4Ni-4Cu alloy in long-term aging at 475 °C

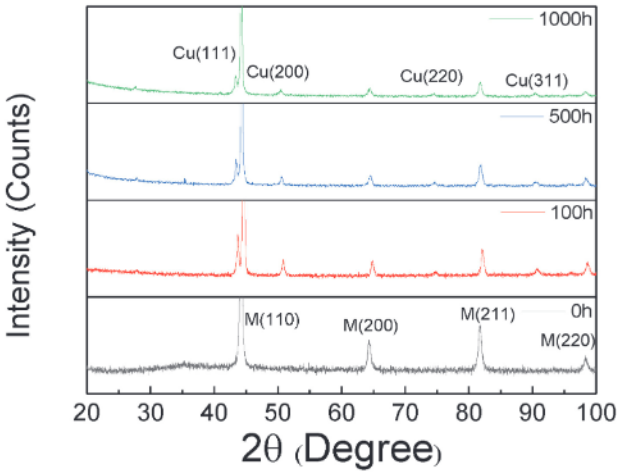

Figure 2: The XRD profile of Fe-17Cr-4Ni-4Cu alloy aged at 475 °C

Figure 3: Optical metallograph obtained from the solution-treated Fe-17Cr-4Ni-4Cu alloy

360 h, with a subsequent decrease in hardness after aging for 1000 h.[16] This, however, is in disagreement with results reported by Hsiao.[17]

3.2 Microstructural evolution during aging

The XRD results of the different aged samples are presented in **Figure 2**. The solution-treated sample shows a BCT lattice, indicating the formation of martensite. However, with an increase in ageing time, copper atoms started clustering and forming precipitates. The formation of Cu-rich precipitates could be detected in the 100-h-aged sample. The XRD does not show any peak due to the precipitates except that for copper.

After solution-treated treatments, the corresponding microstructure of the Fe-17Cr-4Ni-4Cu alloy is composed basically of lath martensite. **Figure 3** shows the metallographic structure obtained from the solution-treated Fe-17Cr-4Ni-4Cu alloy. It can be seen that there are two different black and white zones in the matrix. The same hue area is composed of lath-shaped martensite bundles in the same direction. Since the alloy forms lath martensite containing high-density dislocations after solid solution and quenching treatment, the local deformation zone in the lath martensite can not only provide channels for the diffusion of Cu atoms, but also lower the nucleation energy to help the precipitates' nucleation.

A TEM micrograph of the microstructure of Fe-17Cr-4Ni-4Cu alloy after aging for about 500 h at 475 °C is shown in **Figure 5**. Further evidence for the spinodal decomposition of the martensite phase (white arrow in **Figure 5a**) is seen. The fine-scale spinodal decomposition of α-ferrite results in Cr-rich bright image

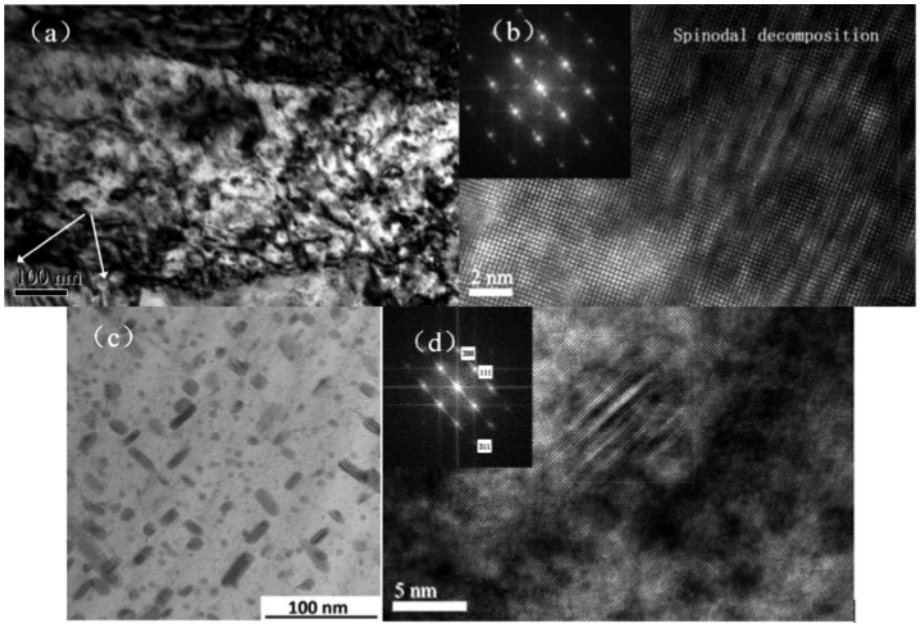

Figure 4: TEM images of the alloy after aging 100 h at 475 °C: a) image of spinodal decomposition structure (arrowed), b) HREM of spinodal zone, c) the precipitation of Cu, d) HREM of a Cu precipitate

domains and Fe-rich dark image domains. **Figure 5b** shows a HREM image and the corresponding Fourier transform obtained from **Figure 5a**. As shown in **Figure 5b**, after aging 500 h, the phase interface between the rich-Cr α' phase and the Fe-rich α phase has gradually become clear, indicating that the decomposition has been fully carried out and reached the phase-equilibrium state. From the results of the Fourier transform, there is a BCC matrix. The main precipitation identified in the Fe-17Cr-4Ni-4Cu alloy at this stage was Cu-rich precipitates with a size of about 30 nm, as shown in **Figure 5c**, which is obviously larger than that seen in the condition aged 100 h at 475 °C (**Figure 4c**). It is ascribed to the coarsening of Cu-rich precipitates under the condition of the longer aging time, namely, Ostwald ripened Cu-rich precipitates. Most precipitates were close to spherical in shape, with very small precipitates being slightly elongated. **Figure 5d** show HREM micrographs of typical copper precipitates. The sizes of the precipitates shown in **Figure 5d** are 4–6.0 nm. Most exhibit the characteristic herring-bone fringe pattern which allows the immediate identification of a twinned 9R structure.[19,20] They are similar to those found previously in thermally-aged 17-4PH steel.[17,21] The fringe periodicity, measured across several fringes, have a spacing of about three times the expected (001) 9R close-packed plane spacing, which is approximately 0.6 nm. The angle between the fringes in adjacent twin segments is approximately 122°. This value is smaller than the angle of 129° characteristic for the orientation relationship found in precipitates immediately after the BCC→9R martensitic transformation in thermally aged alloys, and suggests that rotations of the (009)9R planes have occurred. It is well known that the precipitation of Cr-rich α' by spinodal decomposition is the main cause of the hardening behavior in this stage.[18,22,23] However, hardening effects in this stage was weakened by the Ostwald ripening of the Cu-rich precipitates. Hence, the hardening behavior in this stage is the net result of strengthening by the precipitation of α' and weakening by the Ostwald ripening of the Cu-rich precipitates. So the hardness of the alloy increases slowly.

Figure 6 is a TEM micrograph of the microstructure of the Fe-17Cr-4Ni-4Cu model alloy after aging about

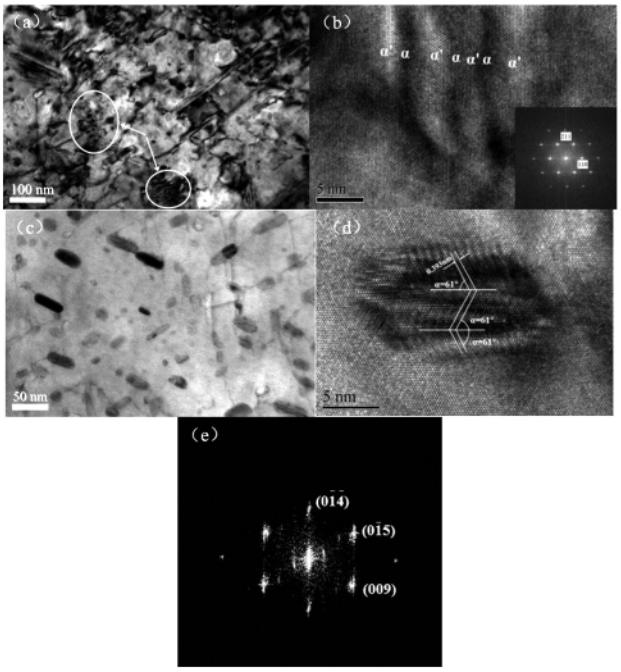

Figure 5: TEM images of the alloy after aging 500 h at 475 °C: a) image of spinodal decomposition structure (arrowed), b) HREM of spinodal zone, c) precipitation of Cu-rich phase, d) HREM showing herring-bone fringe pattern with a twinned 9R structure within the Cu-rich precipitate, e) Fourier transform of (d) lattice image

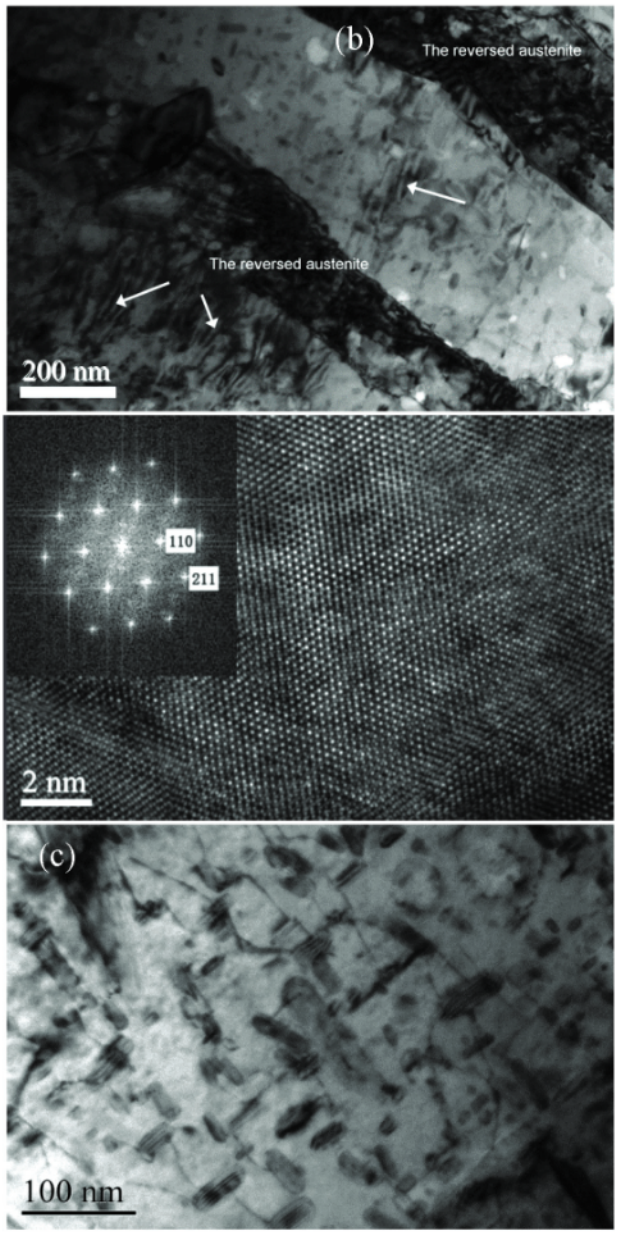

Figure 6: TEM images of the model alloy after aging 1000 h at 475°C: a) image of spinodal decomposition structure (arrowed) and the reversed austenite, b) HREM of spinodal zone, c) precipitation of ε-copper

1000 h at 475 °C. There is a great deal of spinodally decomposed microstructure that is mainly distributed near the grain boundary in **Figure 6a** (white arrowed). By comparing **Figure 4a** and **Figure 6a**, it is clear that the spinodal decomposition occurs first at the grain boundaries (GB). Ramanarayan ascribes this to the fact that the grain boundaries have higher free energy and the atoms adjacent to the grain boundaries have relatively higher mobility.[24] **Figure 6b** shows the HREM lattice image and the corresponding Fourier-transform structure analysis of ferrite matrix. In the ferrite matrix along [001] direction, there were two kinds of fringes cross on projected plane as shown in **Figure 6b**. Fourier transform of this lattice image indicated that the spots were the diffraction pattern of ferrite (BCC) (**Figure 6b**). These two kinds of fringes are the families of (110). Moreover, substantial reversed austenite is present in **Figure 6a**. This shows that the Fe-17Cr-4Ni-4Cu alloy produces inverted austenite, which is distributed at the boundary of martensite lath, after aging about 1000 h at 475 °C. This is because the atoms are easy to diffuse at the lath boundary, and a large number of alloy elements are enriched at the lath boundary during aging, which provides favorable conditions for the transformation and stabilization of reversed austenite. The hardness of the austenite is much less than that of the martensite, so the hardness of alloy now decreases. Even the presence of the α' precipitate cannot make up for this decrease, so the net effect during this stage of the aging is softening (**Figure 1**). Moreover, a large number of the ripening ε-copper precipitates with a size of 40 nm appear, as shown in **Figure 6c**. It leads to loss of coherency with the matrix, which is another contributor to the hardness decline.

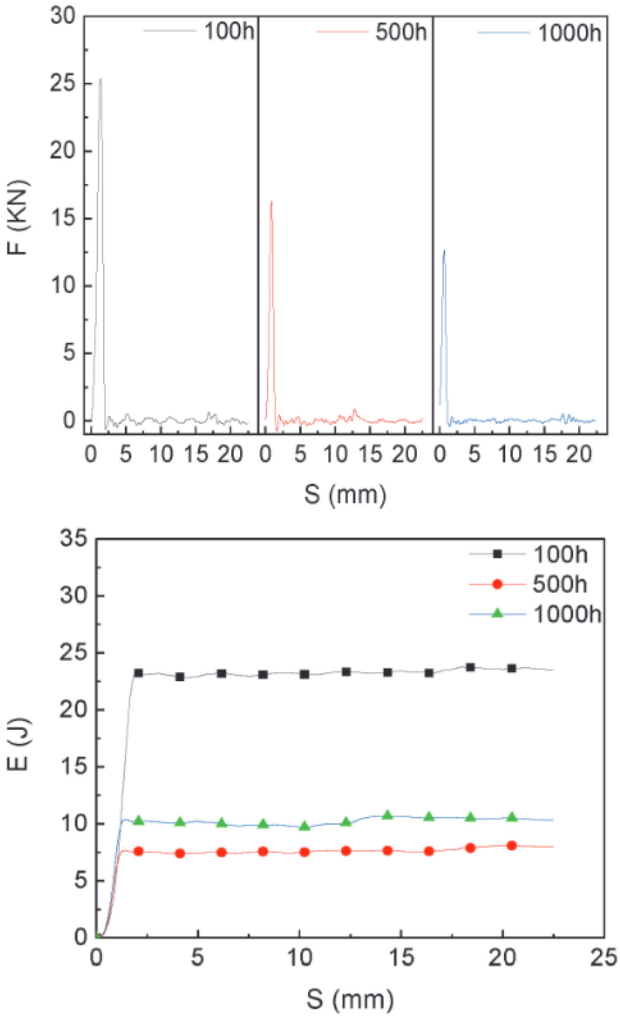

Figure 7: Instrumented Charpy impact load-absorbed energy curves of Fe-17Cr-4Ni-4Cu alloy aging at 475 °C

3.3 Impact test results

Load–displacement diagrams of the impact loading take into account the substructural non-uniformity of the Fe-17Cr-4Ni-4Cu alloy components (microlevel), peculiarities of deformation of structural element conglomerates (meso-level), and allow dividing the energy at the stages of crack initiation and propagation (macrolevel). **Figure 7** shows the instrumented Charpy impact curve of the model alloy aged at 475 °C for (100, 500 and 1000) h, respectively. It can be seen from **Figure 7a** that the work of steady crack propagation during fracture is about zero, and the elastic deformation work is large for the aging temperature of 475 °C. In the elastic deformation stage, the brittle unstable propagation of the crack occurs, indicating that the entire sample has obvious brittle behavior. This is mainly due to the formation of Cr-rich α' phase during aging process, which will lead to many microcracks in different positions of the alloy. At the same time, there are also ε-Cu particles in the model alloy. It is easy to form micro pores during the impact process, and a large number of micro pores will also form micro cracks. Once the micro cracks are formed, the instability and expansion will occur rapidly, resulting in brittle fracture of the material.[25,26] It can be seen from **Figure 7b** that the total impact absorbed energy first decreases and then increases with the increase of aging time, which is consistent with the change trend of hardness in **Figure 1**.

Impact toughness can represent the notch sensitivity of the material and evaluate the resistance of a material to impact load under the condition of stress concentration.[27,28] Crack initiation work (W_i), crack propagation work (W_p) and total impact energy (W_t) are three internal energy indexes that affect the toughness and brittleness of materials. Theoretically, it is believed that the crack forms at the maximum strength, so the energy absorbed by the maximum load point is used as the crack initiation work (W_i) in this paper. **Table 1** shows the three internal energy indexes W_i, W_p and W_t obtained from the instrumented Charpy impact test. For the same material, the greater the crack propagation work (W_p), the higher the energy consumed by crack propagation, and the better its toughness. When aging at 475 °C, with the increase of

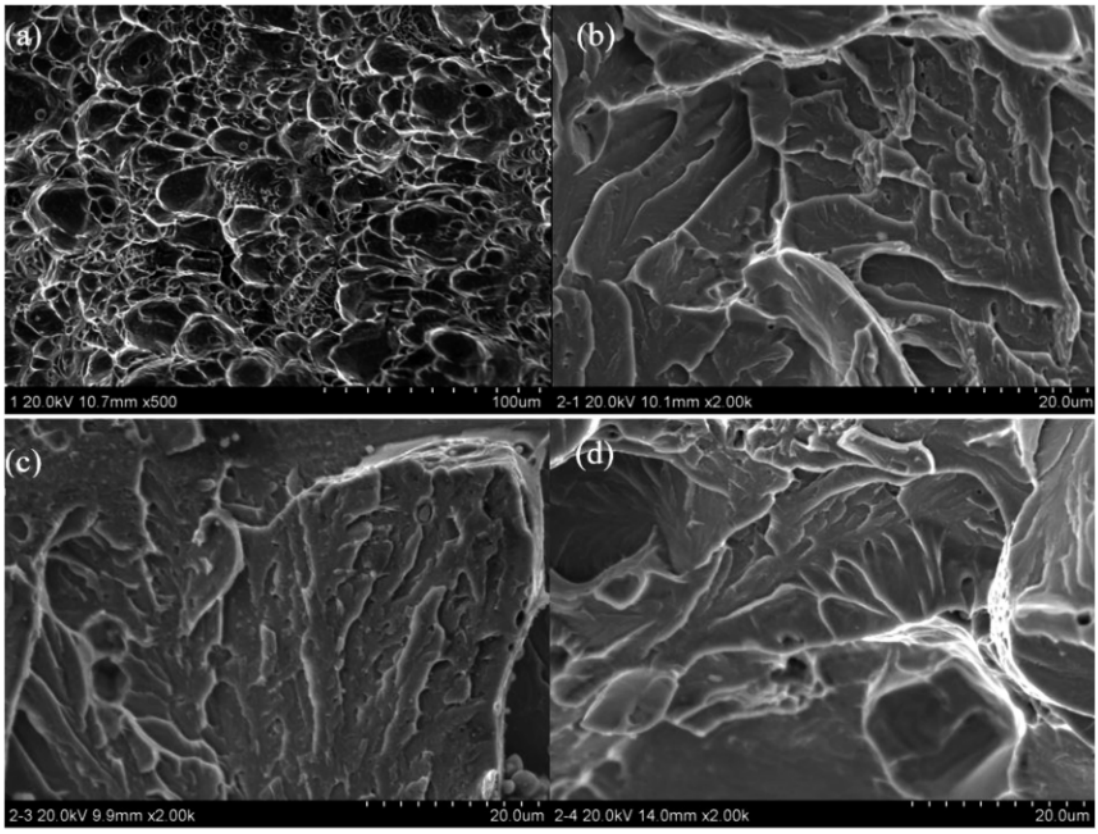

Figure 8: Fracture surface after impact tests of Fe-17Cr-4Ni-4Cu alloy at 20 °C: a) unaged specimen, b) aging at 475 °C for 100 h, c) aging at 475 °C for 500 h, d) aging at 475 °C for 1000 h

aging time, the values of W_i, W_p and W_t first increase, then decrease. It is indicated that the brittleness of the material decreases while the toughness increases continuously, which is consistent with the changing trend of the hardness in **Figure 1**.

Table 1: Crack initiation work (W_i), crack propagation work (W_p) and total impact energy (W_t) obtained from aging at 475 °C

Aging time (h)	W_i/J	W_p/J	W_t/J
100	26.53	71.37	97.9
500	4.47	4.05	4.6
1000	6.1	9.52	10.7

Figure 8 shows the fracture surfaces at the micro-level from the impact tests for the Fe-17Cr-4Ni-4Cu alloy aged at 475 °C after different aging times. In the unaged specimen, the ductile fracture mechanism is dominant, as shown in **Figure 8a**, where a large number of deep dimples can be observed. After an aging time of 100 h, river patterns and a large number of cleavage steps can be observed in the fracture morphology (**Figure 8b**). For 500 h and 1000 h (**Figures 8c** and **8d**), cleavage steps with large distribution range can be seen in the fracture morphology. The fracture surface of the specimens shows predominant quasi-cleavage areas, suggesting that the brittle fracture mechanism has become dominant. However, a few large dimples reappear after an aging time of 1000 h. It is indicated that as the aging time increases, the brittleness of the alloy is weakened. This is because the formation of inversed austenite makes the alloy regain a certain toughness. The conclusion is consistent with the above hardness changes of the Fe-17Cr-4Ni-4Cu alloy.

4 CONCUSIONS

The effect of microstructural evolution on the hardening behavior of the Fe-17Cr-4Ni-4Cu alloy aged at 475 °C can be summarized as follows:

The initial microstructure following solution treatment consists of lath martensite. When the alloy is aged for 100 h at 475 °C, the precipitated Cu-rich phases from the martensite and Cr-rich α'-phase by spinodal decomposition along the grain boundaries lead to a significant increase in hardness together. Continued aging to 500 h leads to the increased precipitation of the Cr-rich α', which provides significant strengthening, reaching maximum hardening despite the continued loss of hardening by weakening by the Ostwald ripening of the Cu-rich precipitates. Extending the aging time to 1000 h leads to substantial reversed austenite transformation and a large number of the ripening ε-copper precipitates that causes softening. The hardness of alloy now decreases. The results of the instrumented Charpy impact tests show that

the impact toughness of model alloy aging at 475 °C drastically drops with the increase of the aging time. Based on the SEM observations, it is concluded that the major fracture mode is cleavage and/or quasi-cleavage.

Acknowledgment

This work was supported by National Key R&D Program of China (2017YFA0403704); Innovation talent Project of colleges and universities in Liaoning Province in 2020; Shenyang Young and Middle-aged Science and Technology Innovation Talents Project (RC200355) in Liaoning Province; Leading scientific research projects of China National Nuclear Corporation (LC202309000301).

5 REFERENCES

[1] H. L. Gao, Y. Liang, H. Wang, B. Hu, Effect of Aging processes on Mechanical Property and Microstructure of 17-4PH Stainless Steel, Heat Treatment, 34 (**2019**) 1, 36–38, doi:10.3969/j.issn.1008-1690.2019.01.009

[2] D. W. Deng, R. Chen, X. Tian, D. Y. Wang, Influence of heat treatment on microstructure and properties of 17-4PH martensitic stainless steel, Heat Treatment of Metals, 38(**2013**) 4, 32–36, doi:10.13251/j.issn.0254-6051.2013.04.013

[3] H. X. Wang, J. Hu, J. Bao, Y. M. Wu, Effect of Chemical composition and Heat Treatment Process on Mechanical Properties of Steel 17-4PH, Special Steel Technology, 14 (**2008**) 2, 26–30, doi:10.16883/j.cnki.issn1674-0971.2008.02.005

[4] C. R. Das, A. K. Bhaduri, S. K. Albert, Characterisation of microstructure and its effect on the strength and toughness of 17-4PH stainless steel, Int. J. Nuclear Energy Science and Technology, 4 (**2009**) 4, 355–365, doi:10.1504/ijnest.2009.028601

[5] P. J. Grobner, The 885 °F (475°C) embrittlement of ferritic stainless steels, Metallurgical and Materials Transactions B, 4 (**1973**) 1, 251–260, doi:10.1007/BF02649625

[6] F. Danoix, P. Auger, Atom Probe Studies of the Fe–Cr System and Stainless Steels Aged at Intermediate Temperature: A Review, Materials Characterization, 44 (**2000**) 1, 177–201, doi:10.1016/S1044-5803(99)00048-0

[7] Y. Zhao, Y. H. Guo, K. Hou, Effect of Heat Treatment Processes on Mechanical Properties of 17-4PH Stainless Steel, Materials for Mechanical Engineering, 33 (**2009**) 5, 5–8, doi:10.1016/S1003-6326(09)60084-4

[8] B. Chen, H. F. Chen, Z. M. Wang, Present Situation and Development Trend of 17-4PH Stainless Steel, Journal of Shanghai Institute of Technology (Natural Science), 16 (**2016**) 1, 83–87, doi:10.3969/j.issn.1671-7333.2016.01.014

[9] M. K. Miller, J. M. Hyde, A. Cerezo, G. D. W. Smith, Comparison of low temperature decomposition in Fe-Cr and duplex stainless steels, Applied Surface Science, 87/88 (**1995**), 323–328, doi:10.1016/0169-4332(95)00497-1

[10] X. Xu, J. E. Westraadt, J. Odqvist, T. G. A. Youngs, S. M. King, P. Hedstrom, Effect of heat treatment above the miscibility gap on nanostructure formation due to spinodal decomposition in Fe-52.85 at.%Cr, Acta Materialia, 145 (**2018**), 347–358, doi:10.1016/j.actamat.2017.12.008.

[11] C. N. Hsiao, C. S. Chiou, J. R. Yang, Aging reactions in a 17-4 PH stainless steel, Materials Chemistry & Physicsm, 74 (**2002**), 134–142, doi:10.1016/S0254-0584(01)00460-6

[12] M. Murayama, K. Hono, Y. Katayama, Microstructural evolution in a 17-4 PH stainless steel after aging at 400 °C, Metall. Mater. Trans. A, 30 (**1999**), 345–353, doi:10.1007/s11661-999-0323-2

[13] X. D. Lin, Q. J. Peng, E. H. Han, W. Ke, Review of Thermal Aging of Nuclear Grade Stainless Steels, Journal of Chinese Society for Corrosion and Protection, 37 (**2017**) 2, 81–92, doi:10.11902/1005.4537.2016.073

[14] W. You, J. H. Lee, S. K. Shin, B. H. Choe, U. Paik, J. H. Lee, Embrittlement Fracture in a 17-4 PH Stainless Steel after Aging at 400°C, Materials Science Forum, 516(**2005**) 973, 241-244, doi:10.4028/www.scientific.net/MSF.486-487.241

[15] B. Yrieix, M. Guttmann, Aging between 300 °C and 450°C of wrought martensitic 13-17 wt% Cr stainless steels, Materials Science and Technology, 9 (**1993**) 2, 125–137, doi:10.1179/mst.1993.9.2.125

[16] G. Yeli, M. A. Auger, K. Wilford, G. D. W. Smith, P. A. J. Bagot, M. P. Moody, Sequential nucleation of phases in a 17-4PH steel: Microstructural characterisation and mechanical properties, Acta Materialia, 125 (**2017**), 38–49, doi:10.1016/j.actamat.2016.11.052

[17] C. N. Hsiao, C. S. Chiou, J. R. Yang, Aging reactions in a 17-4 PH stainless steel, Materials Chemistry and Physics, 74 (**2002**) 2, 134–142, doi:10.1016/S0254-0584(01)00460-6

[18] K. L. Weng, H. R. Chen, J. R. Yang, The low-temperature aging embrittlement in a 2205 duplex stainless steel, Materials Science and Engineering A, 379 (**2004**) 1–2, 119–132, doi:10.1016/j.msea.2003.12.051

[19] H. R. H. Bajguirani, M. L. Jenkins, High-resolution electron microscopy analysis of the structure of copper precipitates in a martensitic stainless steel of type PH 15-5, Philosophical Magazine Letters A, 73 (**1996**) 4, 155–162, doi:10.1080/095008396180786

[20] P. J. Othen, M. C. Jenkins, G. D. W. Smith, W. J. Phythian, High-resolution electron microscopy studies of the structure of Cu precipitates in α-Fe, Philosophical Magazine A, 70 (**1994**) 1, 1–24, doi:10.1080/01418619408242533

[21] H. R. H. Bajguirani, The effect of ageing upon the microstructure and mechanical properties of type 15-5PH stainless steel, Materials Science and Engineering A, 338 (**2002**) 1–2, 142–159, doi:10.1016/s0921-5093(02)00062-X

[22] M. Murayama, Y. Katayama, K. Hono, M. Murayama, K. Hono, Y. Katayama, Microstructural evolution in a 17-4 PH stainless steel after aging at 400 °C, Metall. Mater. Trans. A, 30 (**1999**) 2, 345–353, doi:10.1007/s11661-999-0323-2

[23] T. R. Leax, S. S. Brenner, J. A. Spitznagel, Atom probe examination of thermally ages CF8M cast stainless steel, Metallurgical Transactions A, 23 (**1992**) 10, 2725-2736, doi:10.1007/BF02651752

[24] H. Ramanarayan, T. A. Abinandanan, Grain boundary effects on spinodal decomposition: Discontinuous microstructures, Acta Materialia, 52 (**2004**) 4, 921–930, doi:10.1016/j.actamat.2003.10.028

[25] X. W. Li, Z. M. Zhang, X. G. Li, C. G. Kong, K. Guo, Influence of Microstructure on Impact Toughness and Pitting Sensitivity of 17-4PH Martensitic Stainless Steel, Corrosion & Protection 41 (**2020**) 9, 55–59, doi:10.11973/fsyfh-202009010

[26] X. Yang, The properties and microstructures of 17-4 PH stainless steel (Dissertation in Chinese), Harbin Engineering University, (**2007**), doi:10.76666/d.y1211934

[27] A. P. Sorochak, P. O. Maruschak, O. P. Yasniy, T. Vuherer, S. V. Panin, Evaluation of dynamic fracture toughness parameters of locomotive axle steel by instrumented Charpy impact test, Fatigue & Fracture of Engineering Materials & Structures, 40 (**2017**) 4, 512–522, doi:10.1111/ffe.12510

[28] J. H. Pan, Dynamic Fracture Behavior of Pressure Vessel Metal Materials under Impact Loads (Dissertation in Chinese), University of Science and Technology of China, (**2013**), doi:10.7666/d.Y2280182